

THE STRUCTURE OF THE UNIVERSE ON 100 MPC SCALES

JAAN EINASTO

Tartu Observatory, EE-61602, Estonia

Observational evidence for the presence of a preferred scale around 100 Mpc in the distribution of high-density regions in the Universe is summarised. Toy models with various degrees of regularity are analysed to understand better the observational data. Predictions of models which produce a feature on the initial power spectrum of matter are analysed and compared with new observational data on the CMB angular spectrum, cluster mass function, and galaxy and cluster power spectrum.

1 Introduction

Until the mid-1970s the astronomical community accepted the paradigm that galaxies are distributed in space more or less randomly and that about 5 – 10 % of all galaxies are located in clusters which are also randomly distributed. A paradigm change occurred during a Symposium on Large-Scale Structure of the Universe in 1977 in Tallinn. Several teams reported results of studies of the 3-dimensional distribution of galaxies in superclusters, and demonstrated that superclusters consist of chains (filaments) of galaxies, groups and clusters, and that the space between galaxy systems is devoid of any visible galaxies (Jõeveer & Einasto 1978, Tarenghi *et al.* 1978, Tift & Gregory 1978, Tully & Fisher 1978).

The discovery of the filamentary character of superclusters and the presence of large empty voids made obsolete the early theories of structure formation – the hierarchical clustering model by Peebles (1980), and the whirl theory by Ozernoy (1978). The first impression was that the winning theory was the pancake scenario by Zeldovich (1978). However, a more detailed analysis has shown that the original pancake scenario also has weak points – the structure forms too late and has no fine structure of faint galaxy filaments in large voids (Zeldovich, Einasto & Shandarin 1982). Then the Cold Dark Matter model was suggested and generally accepted (Blumenthal *et al.* 1984). Recently it was replaced by a CDM model dominated by a cosmological term (vacuum energy) – the LCDM model. However, this model has also at least one weak point: in LCDM model superclusters are randomly distributed, whereas observational evidence suggests that rich superclusters and voids form a quasi-regular network of scale $\sim 100 - 130 h^{-1}$ Mpc (Einasto *et al.* 1997a, 1997d). Here we use the dimensionless Hubble constant h defined as $H_0 = 100 h \text{ km s}^{-1} \text{ Mpc}^{-1}$. These data raise the question: Is the regularity of the distribution of superclusters a challenge for CDM models? My lecture tries to answer this question. First I shall summarise the observational evidence for the presence of the $130 h^{-1}$ Mpc scale, thereafter I shall discuss attempts to explain the presence of this scale theoretically.

2 Evidence for the 100 – 130 Mpc Scale

The evidence for the presence of a scale in the distribution of superclusters has accumulated slowly. Zeldovich, Einasto & Shandarin (1982) noticed that voids

between superclusters have mean diameters about $100 h^{-1}$ Mpc. Kopylov et al. (1988) calculated the cluster correlation function and found a secondary peak at $\sim 125 h^{-1}$ Mpc, which corresponds to superclusters on opposite sides of large voids. Using a slightly different method Mo et al. (1992) confirmed the presence of a feature in the cluster correlation function at $\sim 125 h^{-1}$ Mpc.

The most dramatic demonstration of the scale was made by Broadhurst, *et al.* (1990) who measured redshifts of distant galaxies in a pencil beam directed toward Northern and Southern galactic poles. Their data show that high-density regions in this direction alternate with low-density regions with surprising regularity of a period $\sim 128 h^{-1}$ Mpc. Finally, Einasto et al (1997a, 1997b, 1997d) calculated the cluster correlation function and power spectrum of a 3-dimensional cluster sample and confirmed the presence of a scale of $\sim 120 h^{-1}$ Mpc in the distribution of rich clusters of galaxies.

A similar phenomenon is observed in the distribution of Lyman-break galaxies (Broadhurst & Jaffe 2000) at high redshift, $z \approx 3$. The correlation function of these distant galaxies has secondary peaks. A regularity on a similar scale has been found in the distribution of quasars by Roukema & Mamon (2000). All these data suggest that this scale is primordial and co-moves with the expansion; it can be used as a standard rod.

3 Power Spectrum and Correlation Function of Toy Models

The fluctuating density field can be described by the power spectrum and the correlation function. The power spectrum $P(k)$ characterises the amplitude of density fluctuations for various wavenumbers $k = 2\pi/l$. It is determined by the power indices on large and small scales, n_l , n_s , by the transition scale l_0 (or wavenumber $k_0 = 2\pi/l_0$) and by the amplitude σ_8 on scale $8 h^{-1}$ Mpc. The correlation function $\xi(r)$ characterises the clustering of galaxies or clusters in space; it is defined as the excess probability to find galaxies or clusters over a random distribution of points.

In the ideal case of data not being distorted by errors and being available over the whole space, the power spectrum and the correlation function form mutual pairs of Fourier transformations. In reality they complement each other. We are interested here in the study of the regularity of the structure. To understand better observational data we shall study first several toy models of different geometry. These toy models are: random superclusters, Voronoi tessellation (randomly located void centers, and clusters located between voids as far from void centers as possible), and “regular rod models” (superclusters located randomly along regularly spaced parallel rods oriented along all 3 dimensions). Details of these models were discussed by Einasto et al. (1997c). In all three models clusters within superclusters are generated in an identical way; they are distributed randomly according to an isothermal density law. Thus, on small scales correlation functions and power spectra of all three models are identical. Only on larger scales the models differ. The random supercluster model has no built-in scale and no regularity in the distribution of superclusters. The Voronoi tessellation model has a built-in scale – the mean size of voids, but no regularity in the distribution of superclusters as voids are distributed randomly. The regular rod model has a scale: the spacing of the

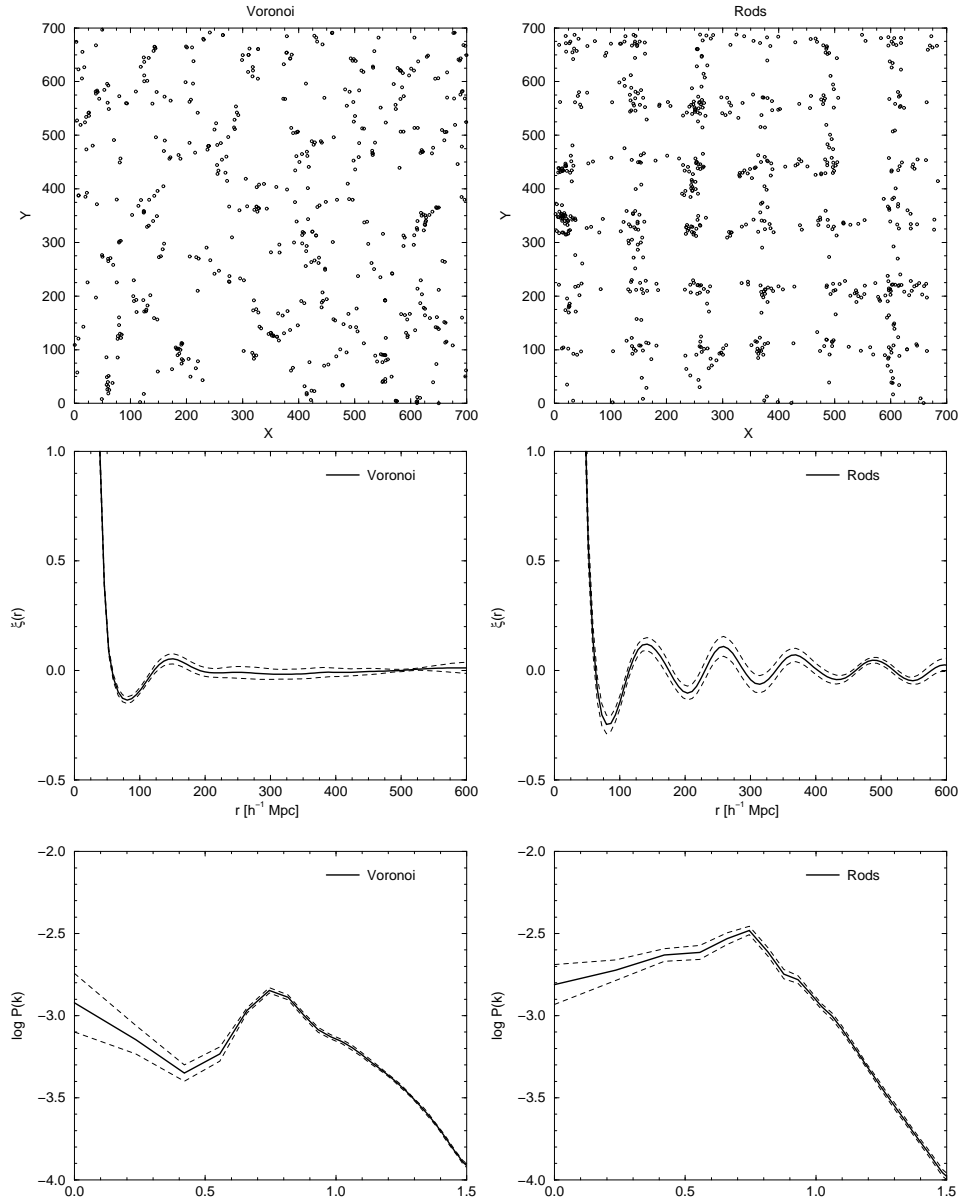


Figure 1. The distribution of clusters in Voronoi and regular rod models (upper left and right panels, respectively), respective correlation functions (middle panels) and power spectra (lower panels). In the lower panels a wavenumber $k = 1$ corresponds to the size of the box in the upper panels.

grid of rods, and also a regularity: the rods form a regular lattice. In Figure 1 we show the distribution of clusters in a sheet of the Voronoi and regular rod models (upper panels), the corresponding correlation functions (middle panels) and power

spectra (lower panels).

The analysis of these toy models allows us to make the following conclusions. On small scales ($r < 50 h^{-1}$ Mpc) the correlation function and power spectrum characterise the distribution of clusters within superclusters, while on larger scales they describe the distribution of superclusters themselves. If superclusters are distributed randomly, then on large scales ($r > 50 h^{-1}$ Mpc) the correlation function is almost zero, $\xi(r) = 0$, and the power spectrum $P(k)$ is flat. The correlation function of the Voronoi model has one secondary minimum and maximum and is zero thereafter, and the power spectrum $P(k)$ has a sharp maximum. The correlation function of the regular rod model is oscillating: it has regularly spaced minima and maxima; the power spectrum has a well-defined sharp maximum on a scale equal to the period of oscillation of the correlation function; it can be approximated by two power law. The position of the maximum of $P(k)$ and the separation of maxima of $\xi(r)$ correspond to the mean diameter of voids and to the separation of superclusters across voids, respectively.

For comparison we can say that all CDM-type models have a smooth power spectrum and a correlation function rather similar to those of the random supercluster model. Here the conflict between observations and model is well seen.

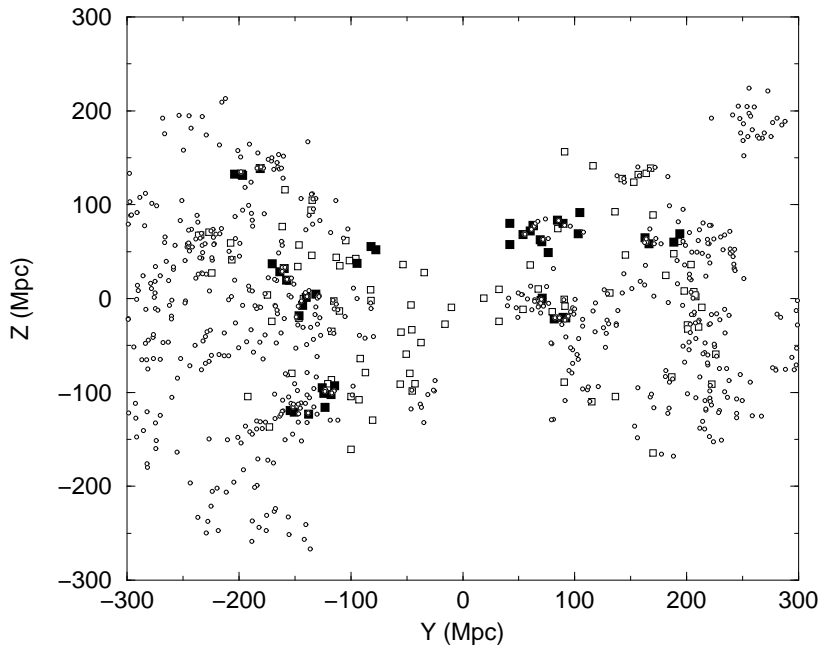


Figure 2. The distribution of Abell clusters (open circles) and X-ray clusters (squares) in supergalactic coordinates. Filled squares denote members of rich superclusters and open squares – isolated X-ray clusters and members of poor systems. In order to minimize the projection effects we plot only Abell clusters from very rich superclusters with at least 8 members.

4 Distribution of Superclusters

4.1 Abell Clusters

We shall use Abell clusters of galaxies as indicators of the distribution of high-density regions in the Universe. The distribution of Abell clusters in rich superclusters is shown in Figure 2 (open circles). We use clusters within a distance limit $350 h^{-1}$ Mpc; the Northern galactic hemisphere is at right, the Southern one at left.

Power spectra of various galaxy and cluster samples are shown in the left panel of Figure 3; the correlation function of Abell clusters in rich superclusters is plotted in the right panel. We see that the correlation function of rich clusters is oscillating with a period $120 h^{-1}$ Mpc. The mean power spectrum of clusters and deep galaxy samples has a sharp maximum on the same wavelength. These properties are similar to properties of the regular rod model.

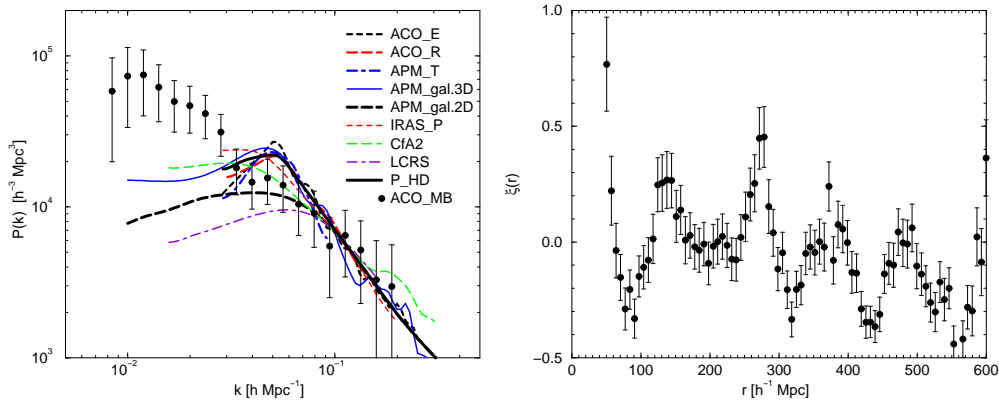


Figure 3. Left: power spectra of galaxies and clusters of galaxies normalized to the amplitude of the 2-D APM galaxy power spectrum (references are given by Einasto *et al.* 1999a). For clarity error bars are not indicated and spectra are shown as smooth curves rather than discrete data points. Bold lines show spectra for cluster data. Points with error bars show the spectrum of Abell clusters by Miller & Batuski (2000) adjusted to the galaxy spectrum amplitude by a relative bias factor $b = 3.2$. Right: correlation function of Abell clusters located in superclusters with at least 8 clusters (Einasto *et al.* 1997b).

4.2 APM and X-ray Clusters

The largest weight in the mean power spectrum plotted in Figure 3 has the Abell cluster sample as it is the deepest and the largest in volume. However, Abell clusters were selected by visual inspection of Palomar survey plates and can be influenced by unknown selection effects. Thus an independent check of the power spectrum and correlation function is needed. We have used A(utomated) P(ate) M(easuring) survey clusters and X-ray selected clusters and active galaxies for comparison.

In Figure 2 we show both optically and X-ray selected clusters, demonstrating that rich superclusters are well seen in both cluster samples. The richest Abell

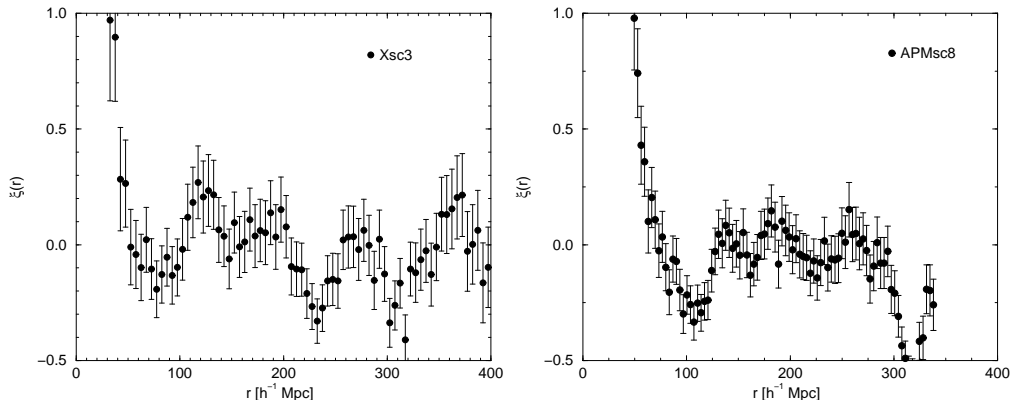


Figure 4. Correlation functions of clusters in rich superclusters: the left panel shows superclusters of richness $N_{cl} \geq 3$ of X-ray selected clusters and active galaxies; the right panel shows superclusters of APM clusters of richness $N_{cl} \geq 8$.

cluster superclusters are also rich in X-ray clusters. There exist differences in detail: not all Abell clusters are strong X-ray emitters, and some X-ray luminous clusters are not included in the Abell catalogue. Similarly, APM clusters do not coincide always with Abell clusters in the same volume. However, the comparison of spatial distributions of cluster samples shows that APM and X-ray selected clusters form rich superclusters very close to rich superclusters of Abell clusters.

Correlation functions of APM and X-ray selected clusters in rich superclusters are also rather similar to the correlation function of Abell clusters in rich superclusters: compare Figures 3 and 4. Again, there are differences in details: the correlation functions of APM and X-ray clusters have a secondary maximum at a separation of $r \sim 190 h^{-1}$ Mpc which is absent in the correlation function of the Abell cluster sample. This feature is due to the fact that the APM sample (and partly the X-ray selected sample) is dominated by two very rich superclusters surrounding an exceptionally large void between Horologium-Reticulum and Sculptor superclusters (Einasto *et al.* 1997d), such that the maximum of the correlation function is shifted. On the other hand, the Abell sample contains a dozen very rich superclusters and differences in void diameters cancel each other out. Due to the smaller volume covered, the APM cluster sample is less suitable for large-scale studies.

The observational evidence can be summarised as follows:

- Rich superclusters and voids form a quasi-regular lattice;
- The mean diameter of cells (the mean separation of rich superclusters across voids) is $120 - 130 h^{-1}$ Mpc.

5 Theoretical Implications

5.1 Evolutionary Toy Models

To investigate the formation of a quasiregular cellular structure we have performed numerical simulations of the evolution of a toy model with two-power-law spectrum of index $n_l = 1$ on large scales and $n_s = -2$ on small scales, and a sharp transition at

wavenumber $k = 0.05 h \text{ Mpc}^{-1}$ (Frisch *et al.* 1995). This power spectrum is rather similar to the observed power spectrum. The two-power-law model reproduces well the distribution of rich clusters of galaxies. Clusters form long filamentary superclusters and a quasiregular supercluster-void network. The correlation function and the power spectrum of the two-power-law model approximates well the observed functions. However, this model is phenomenological. Physically motivated models based on Dark Matter and inflation properties are needed for comparison.

5.2 Cold Dark Matter Models with a Bump

The standard high-density CDM model ($\Omega_m = 1$) has a power spectrum very different from observations. On small scales the COBE normalised CDM model has an amplitude of the spectrum which is much higher than the amplitude of the observed power spectrum of galaxies. As discussed above, this is difficult to explain. LCDM models with cosmological term have better agreement with the observed power spectrum, but they lack the feature at the dominant observed scale. The Low-density Mixed Dark Matter model fits better the observed power spectrum, but no feature is present either.

In some variants of the inflation scenario primordial power spectra have a bump or peak. The model suggested by Lesgourgues, Polarski & Starobinsky (1998) has a break in amplitude and peak; the model by Chung *et al.* (1999) has a bump. Parameters of the model are the position and height of the bump (peak). Power spectra of the Starobinsky model are plotted in the upper left panel of Figure 5. Spectra are based on an LCDM model with shape parameter $\Gamma = \Omega_m h = 0.2$, and bump parameters $p = 1$ (no bump) and $p = 0.7$. The upper right panel shows power spectra of an MDM model with cosmological parameters: baryon density $\Omega_b = 0.06$, CDM density $\Omega_c = 0.29$, HDM (neutrino) density $\Omega_n = 0.05$, vacuum energy density $\Omega_\Lambda = 0.60$, and Hubble parameter $h = 0.65$. This set of parameters is rather close to the model suggested by Ostriker & Steinhardt (1995) and confirmed by new data by Burles *et al.* (1999), Riess *et al.* (1998), Perlmutter *et al.* (1998), and Parodi *et al.* (2000) among others. One spectrum corresponds to the conventional MDM model, the other to the model with Chung peak of amplitude $a = 0.3$. Calculations were made with the CMBFAST package by Seljak & Zaldarriaga (1996).

This Figure shows that a Starobinsky model with a bump is in good agreement with earlier observational data on the galaxy and cluster power spectrum but not with the new data by Miller & Batuski (2000). A mixed dark matter model with Chung peak of amplitude $a = 0.3$ is in good agreement with all observational data.

Finally we have checked the Chung model with other independent data. The lower left panel of Figure 5 shows the cluster mass function calculated using the Press & Schechter (1974) algorithm. These calculations show that the model with a bump produces more clusters of high mass. However within observational errors of the cluster mass functions of both models are in agreement with observations. A similar comparison with new CMB measurements is given in the lower right panel of Figure 5. To improve the agreement with CMB data we have used a tilted MDM model with spectral index $n_l = 0.90$ on large scales, keeping all other cosmological

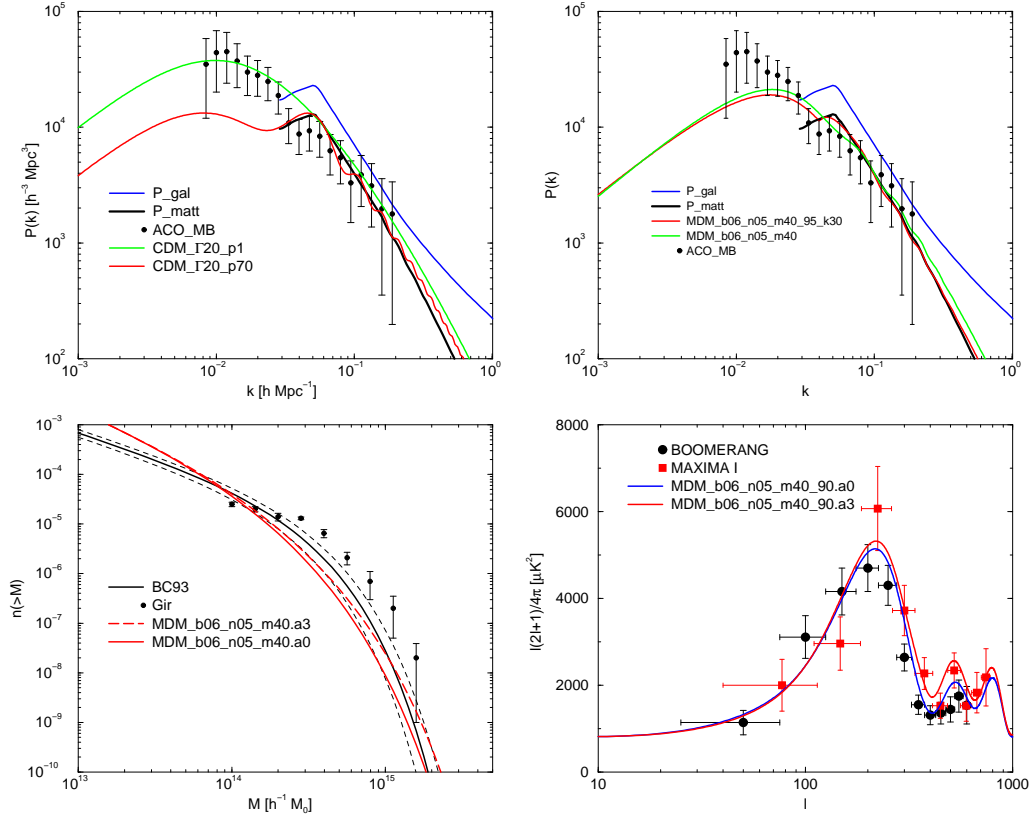


Figure 5. Upper left: power spectra of an LCDM model with and without Starobinsky modification. Upper right: power spectra of MDM models with and without Chung modification. Lower left: cluster mass distributions for MDM models with and without Chung modification. Observed cluster mass functions are shown according to Bahcall & Cen (1993) and Girardi *et al.* (1998). Lower right: angular power spectra of tilted MDM models with and without Chung modification (amplitude parameter $a = 0.3$), compared with BOOMERANG (de Bernardis *et al.* 2000) and MAXIMA I (Hanani *et al.* 2000) data.

parameters as in the model shown in the lower left panel. These calculations show that models with and without the Chung modification are in satisfactory agreement with the CMB angular spectrum. Thus we conclude that this model represents well all available observational data.

However, there are several problems not solved yet. First, the observational question: How large is the region of the regular supercluster-void network? Then the question concerning the interpretation of models: How are spectral features (bump) and regularity related? We hope that this question can be answered with numerical simulations of LCDM models with and without a bump in the power spectrum, and such simulations are under way. Finally, the theoretical questions: Why is there a preferred scale and why does it have a value of $\sim 130 h^{-1} \text{ Mpc}$? What does the presence of a scale and a regularity tell us on the inflation?

6 Conclusions

- There exists good evidence on the presence of a scale of $\sim 130 h^{-1}$ Mpc: it measures the mean distance between rich superclusters across voids.
- There are variants of the inflation scenario suggesting the presence of a characteristic scale (bump) in the power spectrum.
- Models with a bump in the power spectrum are in agreement with other cosmological data using sets of parameters within acceptable ranges.
- Cellular large-scale structure may be the end of the fractal structure of the Universe, as suggested by Ruffini, Song & Taraglio (1988).

We should note that models neither predict the position of the bump, nor the presence and extent of the regularity of the supercluster-void network. We should remember the maxim by Eddington: *no experimental result can be taken seriously if not explained theoretically*. Thus larger surveys are needed to clarify properties of the supercluster-void network. Also a further theoretical analysis are needed to find the physical origin of the scale and the extent of the regularity.

Acknowledgments

I thank Maret Einasto, Mirt Gramann, Pekka Heinamäki, Volker Müller, Enn Saar, Aleksei Starobinsky, Ivan Suhhonenko and Erik Tago for fruitful collaboration and permission to use joint results in this talk. Heinz Andernach kindly improved the presentation. This study was supported by the Estonian Science Foundation grant 2625.

References

1. Bahcall, N.A., & Cen, R., 1993, *Astrophys. J.* **407**, L 49
2. Blumenthal, G.R., Faber, S.M., Primack, J.R. & Rees, M.J., 1984, *Nature* **311**, 517
3. Broadhurst, T. J., Ellis, R. S., Koo, D. C., & Szalay, A. S., 1990, *Nature* **343**, 726
4. Broadhurst, T. J., & Jaffe, A.H., 2000, in *Clustering at High Redshift*, ASP Conf. Ser. 200, eds. A. Mazure et al., p. 241, astro-ph/9904348
5. Burles, S., Nolett, K.M., Truran, J.N., & Turner, M.S., 1999, *Phys. Rev. Lett.* **82**, 4176
6. Chung, D.J.H., Kolb, E.W., Riotto, A., & Tkachev, I.I., 1999, hep-ph/9910437
7. de Bernardis, P. *et al.* , 2000, *Nature* **404**, 955
8. Einasto, J., Einasto, M., Gottlöber, S., Müller, V., Saar, V., Starobinsky, A. A., Tago, E., Tucker, D., Andernach, H., & Frisch, P., 1997a, *Nature* **385**, 139
9. Einasto, J., Einasto, M., Frisch, P., Gottlöber, S., Müller, V., Saar, V., Starobinsky, A.A., Tago, E., Tucker, D., Andernach, H., 1997b, *Mon. Not. R. astr. Soc.* **289**, 801
10. Einasto, J., Einasto, M., Frisch, P., Gottlöber, S., Müller, V., Saar, V., Starobinsky, A.A., Tucker, D., 1997c, *Mon. Not. R. astr. Soc.* **289**, 813

11. Einasto, J., Einasto, M., Tago, E., Starobinsky, A.A., Atrio-Barandela, F., Müller, V., Knebe, A., Frisch, P., Cen, R., Andernach, H., & Tucker, D., 1999a, *Astrophys. J.* **519**, 441
12. Einasto, J., Einasto, M., Tago, E., Müller, V., Knebe, A., Cen, R., Starobinsky, A.A. & Atrio-Barandela, F., 1999b, *Astrophys. J.* **519**, 456
13. Einasto, M., Tago, E., Jaaniste, J., Einasto, J., & Andernach, H., 1997d, *Astron. Astrophys. Suppl.* **123** 119
14. Frisch, P., Einasto, J., Einasto, M., Freudling, W., Fricke, K.J., Gramann, M., Saar, V., & Toomet, O., 1995, *Astron. Astrophys.* **296**, 611
15. Girardi, M., Borgani, S., Giuricin, G., Mardirossian F., & Mezzetti, M., 1998, *Astrophys. J.* **506**, 45
16. Hanany, S., *et al.* , 2000, *Astrophys. J.* (in press), astro-ph/0005123
17. Jöeveer, M., & Einasto, J., 1978, in *The Large Scale Structure of the Universe*, eds. M.S. Longair & J. Einasto, Reidel, p. 241
18. Kopylov, A. I., Kuznetsov D. Y., Fetisova T. S., & Shvarzman V. F., 1988, in *Large Scale Structure of the Universe*, eds. J. Audouze, M.–C. Pelletan, A. Szalay, Kluwer, 129
19. Lesgourgues, J., Polarski, D., & Starobinsky, A. A., 1998, *Mon. Not. R. astr. Soc.* **297**, 769, [astro-ph/9711139]
20. Miller, C. J. & Batuski D.J., 2000, *Astrophys. J.* (in press), astro-ph/0002295
21. Mo, H.J., Deng, Z.G., Xia, X.Y., Schiller, P., & Börner, G., 1992, *Astron. Astrophys.* **257**, 1
22. Ostriker, J.P., & Steinhardt, P.J., 1995, *Nature* **377**, 600
23. Ozernoy, L.M., 1978, in *The Large Scale Structure of the Universe*, eds. M.S. Longair & J. Einasto, Reidel, p. 427
24. Parodi, B.R., Saha, A., Sandage, A., & Tammann, G.A., 2000, *Astrophys. J.* **540**, 634, astro-ph/0004063
25. Peebles, P.J.E.. 1980, *The Large Scale Structure of the Universe*, Princeton: Princeton University Press.
26. Perlmutter, S., *et al.* 1998, *Astrophys. J.* **517**, 565
27. Press, W. H., & Schechter, P. L., 1974, *Astrophys. J.* **187**, 425
28. Riess, A.G., *et al.* 1998, *Astron. J.* **116**, 1009
29. Roukema, B.F., & Mamon, G.A., 2000, *Astron. Astrophys.* **358**, 395, astro-ph/9911413
30. Ruffini, R., Song, D. J. & Taraglio, S., 1988, *Astron. Astrophys.* **190**, 1
31. Seljak, U., & Zaldarriaga, M., 1996, *Astrophys. J.* **469**, 437
32. Tarenghi, M., Tiftt, W.G., Chincarini, G., Rood, H.J. & Thompson, L.A.. 1978, *The Large Scale Structure of the Universe*, eds. M.S. Longair & J. Einasto, Dordrecht: Reidel, p. 263
33. Tiftt, W. G. & Gregory, S.A.. 1978, *The Large Scale Structure of the Universe*, eds. M.S. Longair & J. Einasto, Dordrecht: Reidel, p. 267
34. Tully, R.B. & Fisher, J.R.. 1978, *The Large Scale Structure of the Universe*, eds. M.S. Longair & J. Einasto, Dordrecht: Reidel, p. 214
35. Zeldovich, Ya.B., 1978, *The Large Scale Structure of the Universe*, eds. M.S. Longair & J. Einasto, Dordrecht: Reidel, p. 409
36. Zeldovich, Ya.B., Einasto, J. & Shandarin, S.F., 1982, *Nature* **300**, 407